

Conference Report

Treatment with Akebia Saponin D Ameliorates $A\beta_{1-42}$ -Induced Memory Impairment and Neurotoxicity in Rats

Yongde Chen ¹, Xiaolin Yang ², Tong Chen ¹, Jing Ji ¹, Li Lan ¹, Rong Hu ^{3,*} and Hui Ji ^{1,*}

¹ Department of Pharmacology, China Pharmaceutical University, 24 Tongjia Xiang, Nanjing 210009, Jiangsu, China; chen Yongde1123@163.com (Y.C.); cpu07415chentong@126.com (T.C.); 18061614261@163.com (J.J.); lanliapple@163.com (L.L.)

² College of Pharmacy, Nanjing University of Chinese Medicine, Nanjing 210023, Jiangsu, China; xiaolynsn@126.com

³ State Key Laboratory of Natural Medicines, Department of Physiology, China Pharmaceutical University, 24 Tongjia Xiang, Nanjing 210009, Jiangsu, China

* Correspondence: michelhu@hotmail.com (R.H.); huijicpu@163.com (H.J.); Tel.: +86-137-7082-3968 (R.H.); +86-139-5161-5063 (H.J.)

Academic Editors: Michael Decker and Diego Muñoz-Torrero

Received: 20 January 2016 ; Accepted: 2 March 2016 ; Published: 8 March 2016

Abstract: Amyloid- β peptide ($A\beta$) is known to be directly associated with the progressive neuronal death observed in Alzheimer's disease (AD). However, effective neuroprotective approaches against $A\beta$ neurotoxicity are still unavailable. In the present study, we investigated the protective effects of Akebia saponin D (ASD), a typical compound isolated from the rhizome of *Dipsacus asper* Wall, on $A\beta_{1-42}$ -induced impairment of learning and memory formation and explored the probable underlying molecular mechanisms. We found that treatment with ASD (30, 90 or 270 mg/kg) significantly ameliorated impaired spatial learning and memory in intracerebroventricularly (ICV) $A\beta_{1-42}$ -injected rats, as evidenced by a decrease tendency in escape latency during acquisition trials and improvement in exploratory activities in the probe trial in Morris water maze (MWM). Further study showed that ASD reversed $A\beta_{1-42}$ -induced accumulation of $A\beta_{1-42}$ and $A\beta_{1-40}$ in the hippocampus through down-regulating the expression of BACE and Presenilin 2 accompanied with increased the expression of TACE, IDE and LRP-1. Taken together, our findings suggested that ASD exerted therapeutic effects on $A\beta$ -induced cognitive deficits via amyloidogenic pathway.

Keywords: Alzheimer's disease; Akebia Saponin D (ASD); Amyloid β ($A\beta$)₁₋₄₂; cognitive impairment; neurotoxicity

1. Introduction

Alzheimer's disease (AD) is a multifaceted neurodegenerative disorder featured by progressive memory and cognitive impairment [1–3]. The pathological hallmarks in AD brains are extracellular amyloid plaques composed of aggregated-amyloid ($A\beta$) peptide [4] and abnormally phosphorylated microtubule-associated tau protein [5]. Neurotoxicity $A\beta$ hypothesis of AD. $A\beta$ is derived from sequential endoproteolytic cleavage of a transmembrane $A\beta$ precursor protein (APP) by type 1 transmembrane protein β -site APP cleaving enzyme 1 (BACE1) and γ -secretase complex yielding two major $A\beta$ C-terminal variants, $A\beta_{1-40}$ and $A\beta_{1-42}$ [6–8]. Aggregate $A\beta$ of low molecular weight has been proved to exhibit the greatest neurotoxicity. Alternatively, APP can be subjected to a non-amyloidogenic processing. In the non-amyloidogenic pathway, α -secretase cleavage precludes $A\beta$ generation, releasing a soluble protein called sAPP α [9], which has been reported to have neurotrophic and neuroprotective properties [10,11]. The past decade has witnessed the discovery of

multiple proteases have been shown to be capable of cleaving A β , including neprilysin (NEP) [12,13], insulin-degrading enzyme (IDE) [14,15] and endothelin-converting enzyme-1 (ECE-1) [16,17]. Likely participate in regulating the steady-state levels of A β , IDE, a major soluble protease the degradation of extracellular A β in the brain, is also has the ability to remove the cytoplasmic products of APP. Many studies suggest that IDE expression responds to A β accumulation [18], overexpression of which attenuates brain plaque formation. Conversely, overexpression of IDE attenuates brain plaque formation, prevents premature death in a transgenic AD mouse model [19].

Many studies suggest that prolonged infusion of synthetic A β into the brain can cause learning and memory deficits in animals [20]. However, effective treatment or cure for AD to against A β neurotoxicity is still unavailable yet [21–23]. A complex mixture of herbs In addition, herbal medicines make a valuable contribution to the drug discovery process, the underlying mechanism of action.

Dipsacus asper wall, belonging to Dipsacaceae, is one of the most versatile Chinese herbal drugs usually growing in moist fields and mountain [24,25]. Having been used as a tonic, an analgesic and anti-inflammatory agent for hundreds of years, in the treatment of traumatic hematoma, rheumatic arthritis, bone fractures, low back pain and threaten abortion [26–30]. A previous study Dipsacus asper extract could ameliorate A β_{1-42} -induced cognitive and memory impairment by regulates the level of A β deposition in the hippocampus [31]. Akebia Saponin D (ASD), as a typical compound isolated from the rhizome of Dipsacus asper wall, protect s PC12 cells against amyloid- β induced cytotoxicity [31] and attenuates amyloid β -induced cognitive deficits and inflammatory response in rats. Thus, we hypothesized that ASD therapeutic potential for AD.

In this study, we firstly observed the protective effects of ASD on spatial learning and memory in intracerebroventricularly (ICV) A β_{1-42} -injected rats, and further investigated its possible underlying mechanisms by examining A β generation and degradation pathway.

2. Results

2.1. ASD Reversed Spatial Learning and Memory Impairment Induced by A β_{1-42}

To evaluate the effects of ASD on spatial learning and memory abilities in ICV A β_{1-42} -injected rats, we assessed the performance of rats using Morris water maze. Regardless of different treatments, all the rats displayed progressive decrease in escape latency to reach the hidden platform. Results indicated that ICV A β_{1-42} -injected pronouncedly increased escape latencies compared to the vehicle controls on sessions 2, 3, 4. Interestingly, rat treatment with ASD for four weeks significantly decreased escape latencies compared to the ICV A β_{1-42} -injected group, especially at 90 mg/kg for session 3–4 and 70 mg/kg for session 4 [4 trials/rat/day for 4 days, effect of day, $F(6, 69) = 264.68, p < 0.01$; effect of group, $F(6, 69) = 16.53, p < 0.001$; effect of group-by-day interaction, $F(6, 69) = 2.25, p < 0.001$, Figure 1A]. In addition, the rats in ASD treatment groups also displayed progressive decrease in distance traveled compared to the ICV A β_{1-42} -injected group [effect of day, $F(6, 69) = 557.46, p < 0.001$; effect of group, $F(6, 69) = 17.59, p < 0.001$; effect of group-by-day interaction, $F(6, 69) = 2.92, p < 0.001$, Figure 1B]. In the probe trial, the platform removed from the pool. The time spent in the IV quadrant and the number of platform location crossings was recorded. Rats treatment with ASD significantly increased the time s which were decreased obviously in the model group (Figure 1C), and the distances traveled were significantly increased which were decreased obviously in the model group [effect of group, $F(6, 69) = 13.61$, Figure 1C; effect of group, $F(6, 69) = 29.68$, Figure 1D]. The strategy of searching for the hidden platform was also recorded (Figure 1E). Taken together, our findings suggest that ASD may prevent significantly A β_{1-42} -induced memory impairment in rats.

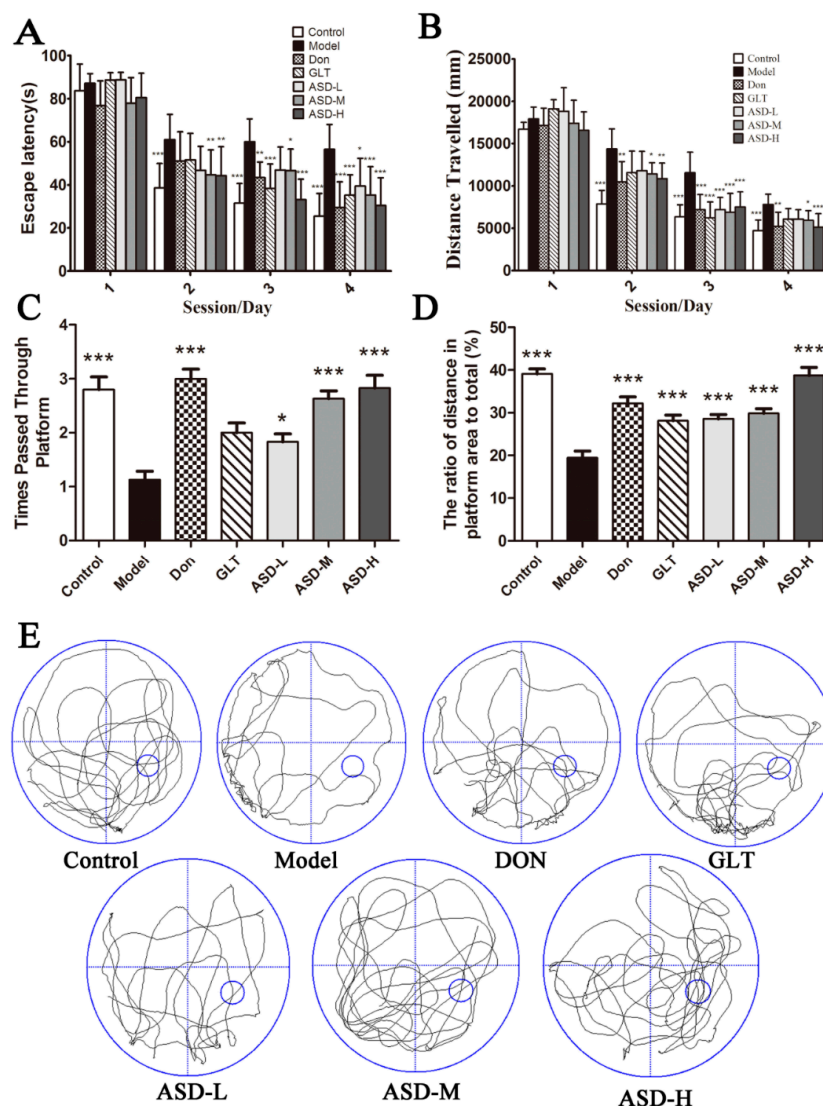


Figure 1. Effects of ASD on the spatial learning and memory deficits in $A\beta_{1-42}$ -induced rats evaluated by Morris water-maze test. (A) Changes in escape latency to reach the hidden platform during the 4-day acquisition trails and (B) distances traveled; (C) The times of former platform location crossings and (D) The ratio of distance in the target quadrant to total moved distance during the probe trial test are presented 24 h after the last acquisition trial; (E) Representative swim paths during the spatial probe test are also shown. Values shown are expressed as means \pm SEM, $n = 10$, * $p < 0.05$, ** $p < 0.01$, *** $p < 0.001$ vs. model group.

2.2. HE Staining

HE staining revealed no remarkable neuronal abnormalities in the hippocampus of rats in the control group. The pyramidal cells in the CA1 region were arranged neatly and tightly, and no cell loss was found. Additionally, for the control group, cells were round and intact with nuclei stained clear, dark blue (Figure 2B). However, obvious hippocampal histopathological damage was observed in the model group. The pyramidal layered structure was disintegrated, and neuronal loss was found in the CA1 region. Neurons with pyknotic nuclei and with shrunken or irregular shape were also observed (Figure 2C). These abnormalities were attenuated by DON, GLT and ASD treatment. The cells in ASD groups had better cell morphology and were more numerous than those in the Model groups, but were overall worse than those in the control group. The average number of healthy cells

was highest in the control group, lower in the treated groups, and lowest in the Model group [effect of group, $F(6, 20) = 17.30$, $p < 0.001$, Figure 2I].

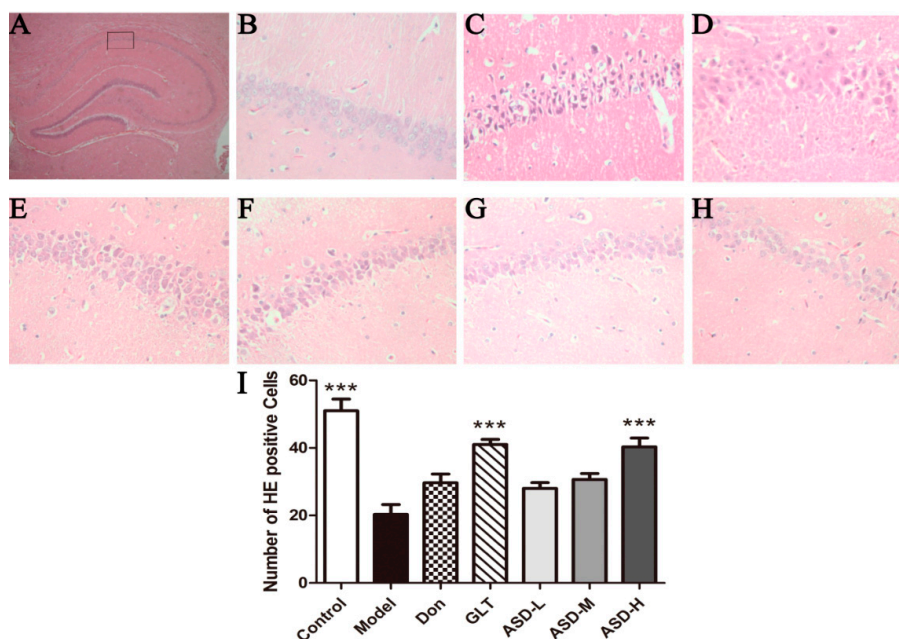


Figure 2. (A) HE staining ($\times 400$). (B) Control group; (C) Model group; (D) DON group; (E) GLT group; (F) ASD-L group; (G) ASD-M group; (H) ASD-H group; (I) Number of positive cells. Rats in control group did not show histopathological abnormalities. In Model and DON groups, cells in the hippocampal CA1 region appeared decreased in number. Furthermore, the remnants of the pyramidal cells were arranged irregularly and some exhibited shrunken and irregular shape. The cells in ASD-H group were more numerous with better cell morphology and were more numerous than those in Model and DON groups, $*** p < 0.001$ vs. model group.

2.3. ASD Blocked $A\beta_{1-42}$ -Induced Production of $A\beta$

To examine the potential mechanisms of ASD, the levels of $A\beta_{1-42}$ and $A\beta_{1-40}$ in hippocampus were measured by ELISA assays. As the result exhibited, there was a rise in concentration of $A\beta_{1-40}$ and $A\beta_{1-42}$ in ICV $A\beta_{1-42}$ -injected group compared to the corresponding vehicle control group. Of note, ASD treatment significantly decreased the level of $A\beta_{1-42}$ and $A\beta_{1-40}$ compared with model group [effect of group, $F(6, 69) = 290.0$, $p < 0.001$, Figure 3A; effect of group, $F(6, 69) = 24.23$, $p < 0.001$, Figure 3B]. As demonstrated by these results, ASD might regulate the generation of $A\beta_{1-40}$ and $A\beta_{1-42}$.

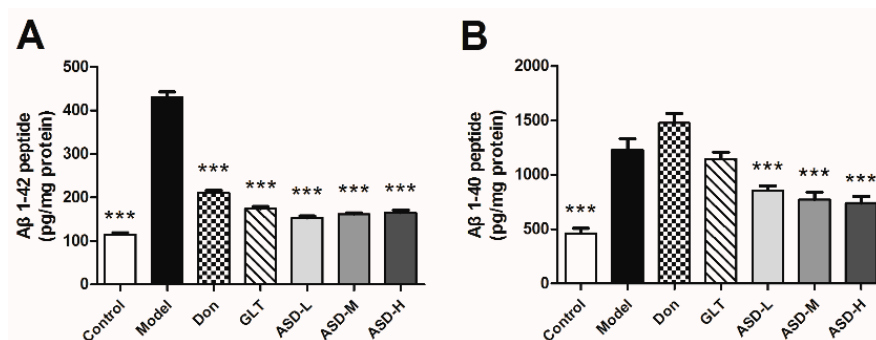


Figure 3. ASD blocked $A\beta_{1-42}$ -induced production of $A\beta$ in the hippocampus of rats. (A) The levels of $A\beta_{1-40}$ and (B) $A\beta_{1-42}$ in this extract were quantified by ELISA assays. Values shown are expressed as means \pm SEM, $n = 10$, $*** p < 0.001$ vs. model group.

2.4. Effects of ASD on the Expression of A β Generation Proteins

To explore the underlying mechanisms of ASD against A β -induced neurotoxicity by down-regulating the generation of A β_{1-42} and A β_{1-40} , we examined the expression of TACE, BACE, presenilin 1 and presenilin 2 by Western blot analyses. As the results exhibited, the expression of TACE was significantly increased in the hippocampus of rats treated with ASD [effect of group, $F(6, 20) = 9.960, p < 0.001$, Figure 4B]. The expression of BACE and presenilin 2 was decreased [effect of group, $F(6, 20) = 13.38, p < 0.001$, Figure 4C; effect of group, $F(6, 20) = 13.38, p < 0.001$, Figure 4E], the expression of presenilin 1 had no significant change [effect of group, $F(6, 20) = 0.1369, p = 0.9889$, Figure 4D].

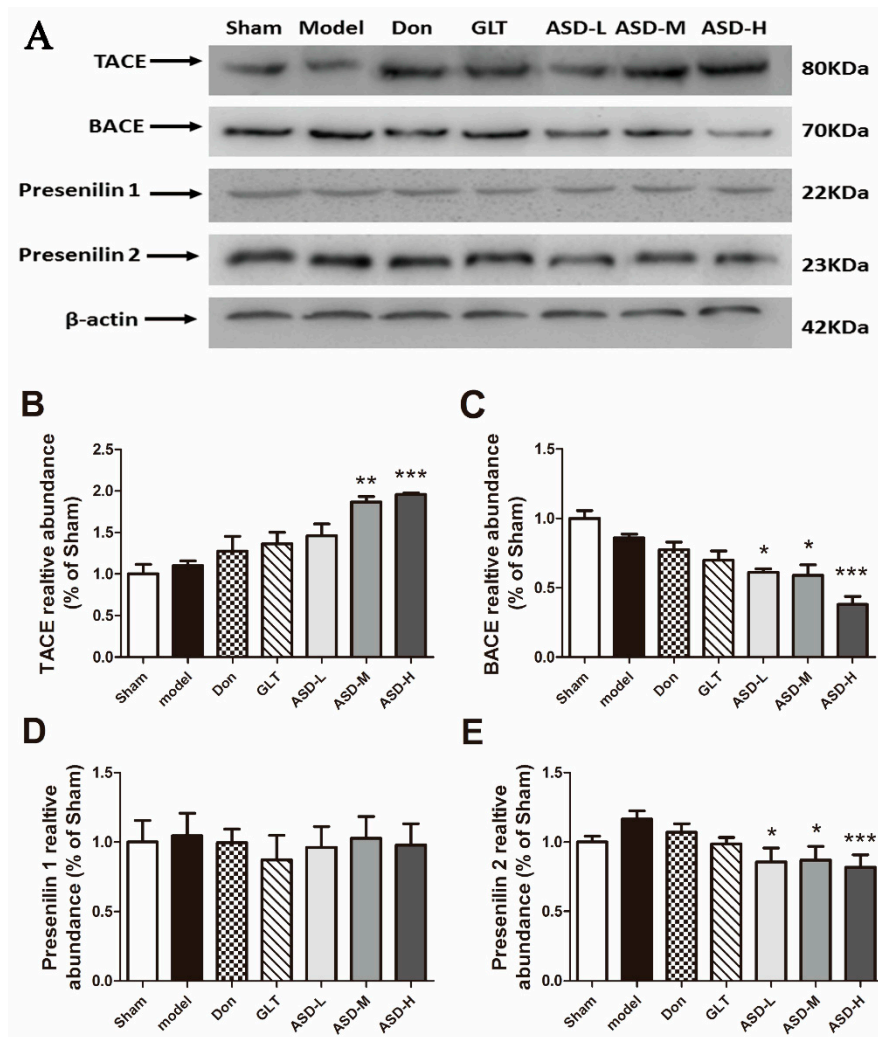


Figure 4. Effects of ASD treatment on the expression of A β generation-related proteins (A) The protein levels of TACE, BACE, Presenilin 1, and Presenilin 2 were detected by western blotting. Quantification of TACE (B); BACE (C); Presenilin 1 (D) and Presenilin 2 (E) was represented as the ratio (in percentage) of the sham group. β -actin was used as a loading control. The data were expressed as mean \pm SEM of three independent experiments, * $p < 0.05$, ** $p < 0.01$, *** $p < 0.001$ vs. hippocampus of vehicle plus A β_{1-42} group.

2.5. Effects of ASD on the Expression of A β Degradation-Related and Transshipment-Related Proteins

To further explore the underlying mechanisms of ASD on A β degradation, we examined the expression of IDE and LRP-1 by Western blot analyses. As shown in Figure 5, ASD significantly increased the expression of IDE and LRP-1 in the hippocampus of rats ($p < 0.05$ or $p < 0.01$, Figure 5A,B).

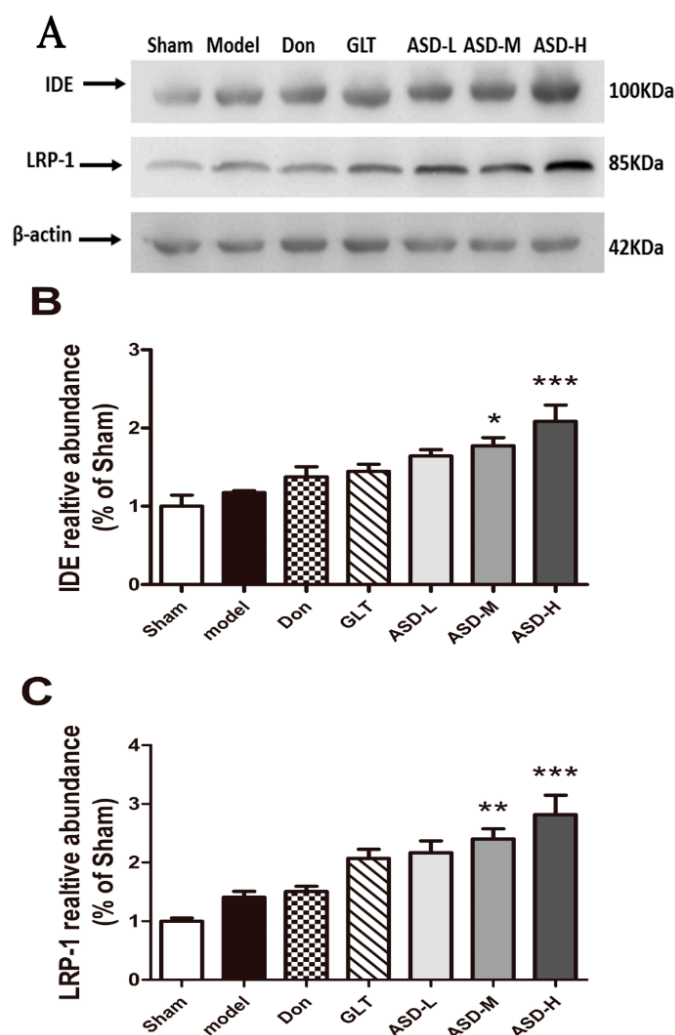


Figure 5. Effects of ASD treatment on the expression of IDE and LRP-1 using western blotting analysis. (A) The protein levels of IDE and LRP-1 were detected by western blotting. Quantification of IDE (B); LRP-1 (C) was expressed as the ratio (in percentage) of the sham group. β -actin was used as a loading control. The data were represented as mean \pm SEM of three independent experiments, * $p < 0.05$, ** $p < 0.01$, *** $p < 0.001$ vs. hippocampus of vehicle plus $A\beta_{1-42}$ group.

3. Materials and Methods

3.1. Animals and Housing

A total of 84 Sprague-Dawley rats of adult male, weighing between 250 and 300 g, were procured from B & K Laboratory Animal Corp. Ltd. Shanghai, China. Throughout the study period, the rats were maintained in accordance with the guidelines of National Institutes of Health Guide for Care and Use of Laboratory Animals (publication no. 85-23, revised 1985). Twelve rats were housed in each cage during the study period and were maintained under standardized conditions (22 ± 1 °C, $60\% \pm 10\%$ humidity, 12 h light/dark cycle). Water was provided ad libitum.

3.2. Drugs and Materials

ASD (Figure 6) was prepared by Professor Zhong-Lin Yang. Isolated from *Dipsacus asperoides* at the Key Laboratory of Modern Chinese Medicines, China Pharmaceutical University, and MALDI-TOF mass spectrometry revealed $>93.4\%$ purity. Commercially $A\beta_{1-42}$ (Invitrogen, Waltham,

MA, USA) was stored at $-20\text{ }^{\circ}\text{C}$, then the peptide was dissolved in sterile normal saline at concentration of $2\text{ }\mu\text{g}/\mu\text{L}$, this solution was incubated at $37\text{ }^{\circ}\text{C}$ for 7 days before the surgery [32].

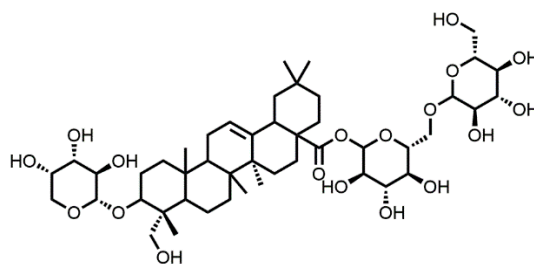


Figure 6. Chemical structure of ASD.

3.3. Stereotaxic Intracerebroventricular (ICV) $A\beta_{1-42}$ Injection and Drug Treatment

The rats were randomly divided into seven groups: Control, Model ($A\beta_{1-42}$), Donepezil ($A\beta_{1-42}$ + 0.5 mg/kg donepezil) as Positive Control 1, Ginkgo leaf tablets ($A\beta_{1-42}$ + 25 mg/kg GLT) as Positive Control 2, ASD-H ($A\beta_{1-42}$ + 270 mg/kg ASD), ASD-M ($A\beta_{1-42}$ + 90 mg/kg ASD) and ASD-L ($A\beta_{1-42}$ + 30 mg/kg ASD). During the surgery, rats were anesthetized with intraperitoneal injection of sodium pentobarbital (30 mg/kg) and then placed on a stereotaxic frame (SR-5, Narishige, Tokyo, Japan). The dura overlying the parietal cortex was exposed. Two burr holes were drilled through the skull in suitable locations according to the stereotaxic atlas of Watson and Paxinos ($A = 3.3\text{ mm}$ caudal to bregma, $L = 2.0\text{ mm}$ lateral to midline, and $V = 2.5\text{ mm}$ below the Dural surface). In the control group, $5\text{ }\mu\text{L}$ sterile normal saline was injected bilaterally at a rate of $1\text{ }\mu\text{L}/\text{min}$ by pump, and in the other groups, $5\text{ }\mu\text{L}$ $A\beta_{1-42}$ ($2\text{ }\mu\text{g}/\mu\text{L}$) was injected bilaterally. The micropipettes were left in place for 5 min to minimize back-flux of liquid [33].

The day of ICV $A\beta_{1-42}$ injection was designated as Day 0. One day after the surgery, rodent feed and sterile distilled water were provided ad libitum. The test group, ASD ($30, 90, 270\text{ mg/kg}$), donepezil (0.5 mg/kg) [34,35] or Ginkgo Biloba Extract (25 mg/kg) were intragastrically administered once daily for consecutive 30 days. In control and model groups the same volume of vehicle as ASD were received.

3.4. Morris Water Maze Task

The Morris water maze task test was conducted to evaluate the spatial learning and memory abilities, which consisted of 4-day training and a probe trial on day 5, carried out from Day 26 to Day 30. This was performed as described previously [36,37]. Rats were individually trained in a black circular pool (150 cm in diameter and 50 cm in height) filled to a depth of 30 cm water with temperature maintained at $25 \pm 1\text{ }^{\circ}\text{C}$. The circular pool was divided into four imaginary quadrants (I, II, III and IV). On each training day (Day 26 to Day 29), the platform always in the middle of IV quadrant (10 cm in diameter) was submerged 1 cm below water and hidden from the rats' view. The animals were subjected to four trials with a 1 h interval between trials. Each trial lasted for 90 s unless the animal reached the platform. If an animal failed to find the platform within 90 s, the test would be ended with the animal being gently navigated to the platform by hand for 30 s. On day 5 (Day 30), the platform was removed and the probe trial was started, during which animals had 90 s to search for the platform. The time spent in the target quadrant and the number of target crossings (*i.e.*, the quadrant where the platform was previously located) was recorded. Data of the escape latency, the time spent in the target quadrant, the number of target crossings and swimming speed were collected by the video tracking equipment and processed by a computer equipped with an analysis-management system (Viewer 2 Tracking Software, Ji Liang Instruments, Shanghai, China).

3.5. Hematoxylin-Eosin Staining of Neurons in the Hippocampus of Rats

On Day 28, following the last treatment, 3 rats of each group were decapitated after injection of a lethal dose of chloral hydrate. The brains were rapidly removed and immersed in 4% formaldehyde for 48 h, then removed and dehydrated in a dehydrator overnight before being embedded in paraffin. Brains were section at a thickness of 5- μ m sections and then baked for 20 min. Subsequently, sections were dewaxed with xylene three times followed by washed with 100%, 95%, 90% and 85% ethyl alcohol solutions for 1 min each and washed with water. Next, sections were stained with hematoxylin, differentiated with hydrochloric acid alcohol solution, treated with 1% ammonia, and stained with eosin for 3 s. After being washed with water, and then 85%, 90%, 95% and 100% ethyl alcohol for 1 min each, sections were cleared in xylene for 2 min and cover-slipped with resin.

3.6. Western Blot Analysis

Rat hippocampi were washed with PBS, chopped off into small pieces, and then homogenized in ice-cold RIPA buffer (Beyotime Institute of Biotechnology Co., Ltd. Haimen, China) containing 0.5% phosphatase inhibitor, 1% phenylmethylsulfonyl fluoride. The homogenate was centrifuged at 12,000 \times g and 4 °C for 15 min the supernatant containing dissolved proteins. Equal amounts of protein were measured using Coomassie bluebased assay kit (Beyotime Institute of Biotechnology Co., Ltd.), t TACE, BACE, presenilin 1, presenilin 2, LRP-1 and IDE. Separated by 10% SDS-polyacrylamide gels, and then transferred onto a PVDF membrane. PVDF membranes were blocked 2 h at room temperature with 5% non-fat milk in Tris-buffered saline with 0.1% Tween 20(TBST). In addition, then the membranes incubated at 4 °C overnight with respective primary antibodies for anti-TACE (1:300, Santa Cruz, Dallas, TX, USA), anti-BACE (1:1000, Cell Signaling Technology, Danvers, MA, USA), anti-presenilin 1 (1:1000, Cell Signaling Technology), anti-presenilin 2 (1:1000, Cell Signaling Technology), anti-IDE (1:1000, Epitomics, Burlingame, CA, USA), anti-LRP1 (1:1000, Epitomics), or anti- β -actin (1:3000, Bioword, Nanjing, China). After washing with TBST three times, the blots were incubated with a horseradish peroxidase conjugated secondary antibody (goat anti-rabbit IgG, 1:50,000, Bioworld Technology Co., Ltd., Nanjing, China) for 2 h at room temperature. After washing with TBST five times, the antibody-reactive bands were visualized by using the enhanced chemiluminescence detection reagents (Tanon Science & Technology Co., Ltd., Shanghai, China) by a gel imaging system (ChemiScope 2850, Clinx Science Instruments Co., Ltd., Shanghai, China). The band intensity analysis was calculated by AlphaEaseFC software (Alpha Innotech, San Leandro, CA, USA).

3.7. Measurement of $A\beta_{1-40}$ and $A\beta_{1-42}$

Rat hippocampi were washed with PBS, chopped off into small pieces, and then homogenized in ice-cold PBS buffer. Containing the homogenate was centrifuged at 12,000 \times g and 4 °C for 15 min. Equal amounts of protein were measured using Coomassie bluebased assay kit (Beyotime Institute of Biotechnology Co., Ltd., Haimen, China). The levels of $A\beta_{1-40}$ and $A\beta_{1-42}$ were assayed using an ELISA kit (Shanghai Jianglai Bioengineering Institute, Co., Ltd., Shanghai, China) according to the manufacturer's protocol. All reactions were performed in triplicates and recorded in 96-well microplates, using a microplate spectrophotometer.

Standard curves were prepared with synthetic $A\beta_{1-42}$ (Bachem, Torrance, CA, USA) diluted in extracts of non-transgenic mouse forebrain prepared in parallel as described above. Each sample was analyzed in duplicate.

3.8. Statistical Analysis

All experimental data shown are expressed as means \pm SD. All the data, unless specified, were analyzed with one-way ANOVA which were followed by Newman-Keuls tests for multiple comparisons using SPSS 11.5 software (SPSS China, Shanghai, China). Statistical significance was considered when $p < 0.05$.

4. Discussion

A primary pathological hallmark of AD is the accumulation of A β in brain [38], which is generated by sequential cleavage from the proteolytic processing of β -amyloid precursor protein (APP). APP generates various peptide species including A β_{1-42} , a more toxic form prone to oligomerize leading to neuroinflammation [39–41], synaptic dysfunction [42,43], apoptosis [44,45] and memory impairment [46], all of which are observed during the progression of AD. One of the important strategies for preventing or treating AD is to interfere with the toxic A β species.

Here, we demonstrated that ASD prevented A β_{1-42} -induced spatial learning and memory impairments, as evidenced by the decrease in escape latency during acquisition trials and improvement in exploratory activities in the probe trial in the MWM task, coupled with modified expression generation-related proteins (TACE, BACE, Presenilin 2), degradation-related proteins (IDE) and transshipment-related proteins (LRP-1).

In this study, rats exposed to 10 μ g amyloid beta (1–42) into the bilateral hippocampus presented a significant impairment in learning and memory ability. In addition, insulin degrading enzyme (IDE), an enzyme involved in A β clearance, can regulate the level of A β in hippocampus. As the results showed, treatment with ASD (90 mg/kg, 270 mg/kg) significantly increased the levels of secreted IDE (* $p < 0.05$, *** $p < 0.001$) and dose-dependently improved the learning and memory deficits induced by A β_{1-42} . In agreement with the experiment data, we hypothesized that ASD might ultimately enhance the levels or activities of secreted IDE which led to induced clearance of A β in the hippocampus. Moreover, A β_{1-40} and A β_{1-42} are produced by the proteolytic processing of APP. Proteases referred to as secretase cleave at the N- and C-termini of A β within APP to generate A β . A previous study showed that the levels of A β_{1-40} is much higher than A β_{1-42} after APP cleavage, we investigated the levels of A β_{1-40} in hippocampus at the same time.

The results indicated that ASD can significantly reduce the levels of A β_{1-40} in hippocampus, along with changes in the levels of A β generate e related enzyme. In conclusion, we hypothesis that ASD regulate the proteolytic processing of APP, mainly regulate the α -secretase, β -secretase or Presenilin 2 to reduce the levels of A β_{1-40} in hippocampus.

In conclusion, we demonstrated that ASD, a saponin separated from *Dipsacus asperwall*, significantly improved the learning and memory abilities impaired by A β injury, protected neurons and markedly regulating A β generate-related proteins (TACE, BACE, Presenilin 2) expression. In addition, we found that ASD might promoted the A β degradation by regulating A β degradation-related proteins (IDE) expression. These findings indicate that ASD might have a therapeutic potential in AD. In the future, In the future, much work requires to be done to demonstrate the effects of ASD on the deposition of amyloid plaques, neurofibrillary tangles and other distinct neuropathological features in AD.

5. Conclusions

In conclusion, the present study has demonstrated for the first time that ASD exerted potently therapeutic effects on A β -induced cognitive deficits via amyloidogenic pathway, as evidenced by a decrease tendency in escape latency during acquisition trials and improvement in exploratory activities in the probe trial in Morris water maze (MWM). Moreover, we firstly found that ASD reversed A β_{1-42} -induced accumulation of A β_{1-42} and A β_{1-40} through down-regulating the expression of BACE and Presenilin 2 accompanied with increased the expression of TACE, IDE and LRP-1.

Acknowledgments: Financial support for the study was provided by grants from the Natural Science Foundation of China (No. 81373419) and the Representational Achievement Cultivating Project of State Key Laboratory of Natural Medicines (SKLNMBZ201402).

Author Contributions: Yongde Chen, Xiaolin Yang and Jing Ji performed animal experiments. Yongde Chen and Li Lan performed cell biology experiments. Yongde Chen and Tong Chen prepared the manuscript. Yongde Chen, Rong Hu and Hui Ji planned the work.

Conflicts of Interest: The authors declare no conflict of interest.

References

1. Mueller, S.G.; Dickerson, B.C. Atrophy accelerates with conversion from mild cognitive impairment to Alzheimer disease. *Neurology* **2008**, *70*, 1728–1729. [[CrossRef](#)] [[PubMed](#)]
2. Querfurth, H.W.; LaFerla, F.M. Alzheimer's disease. *N. Engl. Med.* **2010**, *362*, 329–344. [[CrossRef](#)] [[PubMed](#)]
3. Terry, A.V., Jr.; Callahan, P.M.; Hall, B.; Webster, S.J. Alzheimer's disease and age-related memory decline (preclinical). *Pharmacol. Biochem. Behav.* **2011**, *99*, 190–210. [[CrossRef](#)] [[PubMed](#)]
4. Bero, A.W.; Bauer, A.Q.; Stewart, F.R.; White, B.R.; Cirrito, J.R.; Raichle, M.E.; Culver, J.P.; Holtzman, D.M. Bidirectional relationship between functional connectivity and amyloid-beta deposition in mouse brain. *J. Neurosci.* **2012**, *32*, 4334–4340. [[CrossRef](#)] [[PubMed](#)]
5. Mandelkow, E.M.; Mandelkow, E. Tau in Alzheimer's disease. *Trends Cell Biol.* **1998**, *8*, 425–427. [[CrossRef](#)]
6. Cole, S.L.; Vassar, R. The role of amyloid precursor protein processing by bace1, the beta-secretase, in Alzheimer disease pathophysiology. *J. Biol. Chem.* **2008**, *283*, 29621–29625. [[CrossRef](#)] [[PubMed](#)]
7. Vahidi, A.; Glenn, G.; van der Geer, P. Identification and mutagenesis of the tace and gamma-secretase cleavage sites in the colony-stimulating factor 1 receptor. *Biochem. Biophys. Res. Commun.* **2014**, *450*, 782–787. [[CrossRef](#)] [[PubMed](#)]
8. Wang, Q.; Li, H. Research on regulation function of gamma-secretase inhibitor dapt on the differentiation of neural precursor cell line. *Sheng Wu Yi Xue Gong Cheng Xue Za Zhi* **2015**, *32*, 126–130. [[PubMed](#)]
9. Del Turco, D.; Schlaudraff, J.; Bonin, M.; Deller, T. Upregulation of APP, ADAM10 and ADAM17 in the denervated mouse dentate gyrus. *PLoS ONE* **2014**, *9*, e84962. [[CrossRef](#)] [[PubMed](#)]
10. Bernstein, H.G.; Stricker, R.; Lendeckel, U.; Bertram, I.; Dobrowolny, H.; Steiner, J.; Bogerts, B.; Reiser, G. Reduced neuronal co-localisation of nardilysin and the putative α -secretases ADAM10 and ADAM17 in Alzheimer's disease and down syndrome brains. *AGE* **2009**, *31*, 11–25. [[CrossRef](#)] [[PubMed](#)]
11. Hartl, D.; Klatt, S.; Roch, M.; Konthur, Z.; Klose, J.; Willnow, T.E.; Rohe, M. Soluble Alpha-APP (sAPP α) regulates CDK5 expression and activity in neurons. *PLoS ONE* **2013**, *8*, e65920. [[CrossRef](#)] [[PubMed](#)]
12. Guan, H.; Chow, K.M.; Shah, R.; Rhodes, C.J.; Hersh, L.B. Degradation of islet amyloid polypeptide by neprilysin. *Diabetologia* **2012**, *55*, 2989–2998. [[CrossRef](#)] [[PubMed](#)]
13. Kakiya, N.; Saito, T.; Nilsson, P.; Matsuba, Y.; Tsubuki, S.; Takei, N.; Nawa, H.; Saido, T.C. Cell surface expression of the major amyloid- β peptide ($A\beta$)-degrading enzyme, neprilysin, depends on phosphorylation by mitogen-activated protein kinase/extracellular signal-regulated kinase (mek) and dephosphorylation by protein phosphatase 1a. *J. Biol. Chem.* **2012**, *287*, 29362–29372. [[CrossRef](#)] [[PubMed](#)]
14. Carrasquillo, M.M.; Belbin, O.; Zou, F.; Allen, M.; Ertekin-Taner, N.; Ansari, M.; Wilcox, S.L.; Kashino, M.R.; Ma, L.; Younkin, L.H.; *et al.* Concordant association of insulin degrading enzyme gene (IDE) variants with IDE mRNA, $A\beta$, and Alzheimer's Disease. *PLoS ONE* **2010**, *5*, e8764. [[CrossRef](#)] [[PubMed](#)]
15. Leal, M.C.; Magnani, N.; Villordo, S.; Buslje, C.M.; Evelson, P.; Castano, E.M.; Morelli, L. Transcriptional regulation of insulin-degrading enzyme modulates mitochondrial amyloid β ($A\beta$) peptide catabolism and functionality. *J. Biol. Chem.* **2013**, *288*, 12920–12931. [[CrossRef](#)] [[PubMed](#)]
16. Pacheco-Quinto, J.; Herdt, A.; Eckman, C.B.; Eckman, E.A. Endothelin-converting enzymes and related metalloproteases in Alzheimer's disease. *J. Alzheimers Dis.* **2013**, *33*, S101–S110. [[PubMed](#)]
17. Wang, R.; Wang, S.; Malter, J.S.; Wang, D.S. Effects of 4-hydroxy-nonanal and amyloid- β on expression and activity of endothelin converting enzyme and insulin degrading enzyme in SH-SY5Y cells. *J. Alzheimers Dis.* **2009**, *17*, 489–501. [[PubMed](#)]
18. Vepsalainen, S.; Hiltunen, M.; Helisalmi, S.; Wang, J.; van Groen, T.; Tanila, H.; Soininen, H. Increased expression of $A\beta$ degrading enzyme IDE in the cortex of transgenic mice with Alzheimer's disease-like neuropathology. *Neurosci. Lett.* **2008**, *438*, 216–220. [[CrossRef](#)] [[PubMed](#)]
19. Leissring, M.A.; Farris, W.; Chang, A.Y.; Walsh, D.M.; Wu, X.; Sun, X.; Frosch, M.P.; Selkoe, D.J. Enhanced proteolysis of beta-amyloid in APP transgenic mice prevents plaque formation, secondary pathology, and premature death. *Neuron* **2003**, *40*, 1087–1093. [[CrossRef](#)]
20. Walsh, D.M.; Thulin, E.; Minogue, A.M.; Gustavsson, N.; Pang, E.; Teplow, D.B.; Linse, S. A facile method for expression and purification of the Alzheimer's disease-associated amyloid β -peptide. *FEBS J.* **2009**, *276*, 1266–1281. [[CrossRef](#)] [[PubMed](#)]

21. Folch, J.; Ettcheto, M.; Petrov, D.; Abad, S.; Pedros, I.; Marin, M.; Olloquequi, J.; Camins, A. Review of the advances in treatment for Alzheimer disease: Strategies for combating β -amyloid protein. *Neurologia* **2015**. [[CrossRef](#)]
22. Schenk, D.; Basi, G.S.; Pangalos, M.N. Treatment strategies targeting amyloid beta-protein. *Cold Spring Harb. Perspect. Med.* **2012**, *2*, a006387. [[CrossRef](#)] [[PubMed](#)]
23. Schwartz, A. What's next for alzheimer treatment?: While A β isn't out of the picture yet, several other therapeutic routes are being explored. *Ann. Neurol.* **2013**, *73*, A7–A9. [[CrossRef](#)] [[PubMed](#)]
24. Ginty, D.D.; Bonni, A.; Greenberg, M.E. Nerve growth factor activates a Ras-dependent protein kinase that stimulates c-fos transcription via phosphorylation of CREB. *Cell* **1994**, *77*, 713–725. [[CrossRef](#)]
25. Hung, T.M.; Na, M.; Thuong, P.T.; Su, N.D.; Sok, D.; Song, K.S.; Seong, Y.H.; Bae, K. Antioxidant activity of caffeoyl quinic acid derivatives from the roots of dipsacus asper wall. *J. Ethnopharmacol.* **2006**, *108*, 188–192. [[CrossRef](#)] [[PubMed](#)]
26. Jung, K.Y.; Do, J.C.; Son, K.H. Triterpene glycosides from the roots of dipsacus asper. *J. Nat. Prod.* **1993**, *56*, 1912–1916. [[CrossRef](#)] [[PubMed](#)]
27. Kim, B.S.; Kim, Y.C.; Zadeh, H.; Park, Y.J.; Pi, S.H.; Shin, H.S.; You, H.K. Effects of the dichloromethane fraction of Dipsaci Radix on the osteoblastic differentiation of human alveolar bone marrow-derived mesenchymal stem cells. *Biosci. Biotechnol. Biochem.* **2011**, *75*, 13–19. [[CrossRef](#)] [[PubMed](#)]
28. Niu, Y.; Li, Y.; Huang, H.; Kong, X.; Zhang, R.; Liu, L.; Sun, Y.; Wang, T.; Mei, Q. Asperosaponin VI, a saponin component from Dipsacus asper wall, induces osteoblast differentiation through bone morphogenetic protein-2/p38 and extracellular signal-regulated kinase 1/2 pathway. *Phytother. Res.* **2011**, *25*, 1700–1706. [[CrossRef](#)] [[PubMed](#)]
29. Wang, Y.; Wang, X.X.; Zhang, L.N.; Jin, S.M.; Zhang, J. Effects of traditional chinese medicine on bone remodeling during orthodontic tooth movement. *J. Ethnopharmacol.* **2012**, *141*, 642–646. [[CrossRef](#)] [[PubMed](#)]
30. Zhang, Z.J.; Qian, Y.H.; Hu, H.T.; Yang, J.; Yang, G.D. The herbal medicine dipsacus asper wall extract reduces the cognitive deficits and overexpression of β -amyloid protein induced by aluminum exposure. *Life Sci.* **2003**, *73*, 2443–2454. [[CrossRef](#)]
31. Zhou, Y.Q.; Yang, Z.L.; Xu, L.; Li, P.; Hu, Y.Z. Akebia saponin D, a saponin component from Dipsacus asper wall, protects PC 12 cells against amyloid-beta induced cytotoxicity. *Cell Biol. Int.* **2009**, *33*, 1102–1110. [[CrossRef](#)] [[PubMed](#)]
32. Russo, I.; Caracciolo, L.; Tweedie, D.; Choi, S.H.; Greig, N.H.; Barlati, S.; Bosetti, F. 3,6'-dithiothalidomide, a new TNF- α synthesis inhibitor, attenuates the effect of A β -42 intracerebroventricular injection on hippocampal neurogenesis and memory deficit. *J. Neurochem.* **2012**, *122*, 1181–1192. [[CrossRef](#)] [[PubMed](#)]
33. Yu, X.; Wang, L.N.; Du, Q.M.; Ma, L.; Chen, L.; You, R.; Liu, L.; Ling, J.J.; Yang, Z.L.; Ji, H. Akebia saponin d attenuates amyloid β -induced cognitive deficits and inflammatory response in rats: Involvement of akt/nf-kappab pathway. *Behav. Brain Res.* **2012**, *235*, 200–209. [[CrossRef](#)] [[PubMed](#)]
34. Cummings, J.L.; Geldmacher, D.; Farlow, M.; Sabbagh, M.; Christensen, D.; Betz, P.; Grp, D.M.E.W. High-dose donepezil (23 mg/day) for the treatment of moderate and severe Alzheimer's disease: Drug profile and clinical guidelines. *CNS Neurosci. Ther.* **2013**, *19*, 294–301. [[CrossRef](#)] [[PubMed](#)]
35. Ye, C.Y.; Lei, Y.; Tang, X.C.; Zhang, H.Y. Donepezil attenuates abeta-associated mitochondrial dysfunction and reduces mitochondrial abeta accumulation *in vivo* and *in vitro*. *Neuropharmacology* **2015**, *95*, 29–36. [[CrossRef](#)] [[PubMed](#)]
36. Shi, J.; Liu, Q.; Wang, Y.; Luo, G. Coadministration of huperzine a and ligustrazine phosphate effectively reverses scopolamine-induced amnesia in rats. *Pharmacol. Biochem. Behav.* **2010**, *96*, 449–453. [[CrossRef](#)] [[PubMed](#)]
37. Vorhees, C.V.; Williams, M.T. Morris water maze: Procedures for assessing spatial and related forms of learning and memory. *Nat. Protoc.* **2006**, *1*, 848–858. [[CrossRef](#)] [[PubMed](#)]
38. Glenner, G.G.; Wong, C.W. Alzheimer's Disease and down's syndrome: Sharing of a unique cerebrovascular amyloid fibril protein. *Biochem. Biophys. Res. Commun.* **1984**, *122*, 1131–1135. [[CrossRef](#)]
39. Olkhov, V.K.; Rayburn, S.N. *Leading-Edge Research in Alzheimer's Disease*; Nova Science Publishers: Hauppauge, NY, USA, 2008; pp. 125–131.

40. Candore, G.; Bulati, M.; Caruso, C.; Castiglia, L.; Colonna-Romano, G.; di Bona, D.; Duro, G.; Lio, D.; Matranga, D.; Pellicano, M.; *et al.* Inflammation, cytokines, immune response, apolipoprotein E, cholesterol, and oxidative stress in alzheimer disease: Therapeutic implications. *Rejuven. Res.* **2010**, *13*, 301–313. [[CrossRef](#)] [[PubMed](#)]
41. Abdi, A.; Sadraie, H.; Dargahi, L.; Khalaj, L.; Ahmadiani, A. Apoptosis inhibition can be threatening in A β -induced neuroinflammation, through promoting cell proliferation. *Neurochem. Res.* **2011**, *36*, 39–48. [[CrossRef](#)] [[PubMed](#)]
42. Scip, A.; Tozzi, A.; Abaza, A.; Cardinetti, D.; Colombo, I.; Calabresi, P.; Salmona, M.; Welker, E.; Borsello, T. C-Jun N-terminal kinase has a key role in Alzheimer disease synaptic dysfunction *in vivo*. *Cell Death. Dis.* **2014**, *5*, e1019. [[CrossRef](#)] [[PubMed](#)]
43. Zeng, Y.; Zhao, D.; Xie, C.W. Neurotrophins enhance camkii activity and rescue amyloid-beta-induced deficits in hippocampal synaptic plasticity. *J. Alzheimers Dis.* **2010**, *21*, 823–831. [[PubMed](#)]
44. Gao, C.; Liu, Y.; Jiang, Y.; Ding, J.; Li, L. Geniposide ameliorates learning memory deficits, reduces tau phosphorylation and decreases apoptosis via GSK3 β pathway in streptozotocin-induced alzheimer rat model. *Brain Pathol.* **2014**, *24*, 261–269. [[CrossRef](#)] [[PubMed](#)]
45. Hamdane, M.; Delobel, P.; Sambo, A.V.; Smet, C.; Begard, S.; Violleau, A.; Landrieu, I.; Delacourte, A.; Lippens, G.; Flament, S.; *et al.* Neurofibrillary degeneration of the Alzheimer-type: an alternate pathway to neuronal apoptosis? *Biochem. Pharmacol.* **2003**, *66*, 1619–1625. [[CrossRef](#)]
46. Kostylev, M.A.; Kaufman, A.C.; Nygaard, H.B.; Patel, P.; Haas, L.T.; Gunther, E.C.; Vortmeyer, A.; Strittmatter, S.M. Prion-protein-interacting amyloid-beta oligomers of high molecular weight are tightly correlated with memory impairment in multiple Alzheimer mouse models. *J. Biol. Chem.* **2015**, *290*, 17415–17438. [[CrossRef](#)] [[PubMed](#)]

Sample Availability: Samples of the compound Akebia saponin D is available from Zhong-Lin Yang.



© 2016 by the authors; licensee MDPI, Basel, Switzerland. This article is an open access article distributed under the terms and conditions of the Creative Commons by Attribution (CC-BY) license (<http://creativecommons.org/licenses/by/4.0/>).